Follow-up of solid-state fungal wood pretreatment by a novel near-infrared spectroscopy-based lignin calibration model

Follow-up of solid-state fungal wood pretreatment by a novel near-infrared spectroscopy-based lignin calibration model

Authors

Nikolett Wittner[a], Szilveszter Gergely[b], János Slezsák[b], Waut Broos[a], Siegfried E. Vlaeminck[c], Iris Cornet[a,*]

[a] Research group of Biochemical Wastewater Valorization and Engineering, University of Antwerp, Groenenborgerlaan 171, 2020 Antwerpen, Belgium

[b] Department of Applied Biotechnology and Food Science, Faculty of Chemical Technology and Biotechnology, Budapest University of Technology and Economics, Műegyetem rkp. 3., H-1111 Budapest, Hungary

[c] Research group of Sustainable Energy, Air and Water Technology, University of Antwerp, Groenenborgerlaan 171, 2020 Antwerpen, Belgium

*Corresponding author:

Prof. dr. ir. Iris Cornet

Research group of Biochemical Wastewater Valorization and Engineering

University of Antwerp

Groenenborgerlaan 171

2020 Antwerpen, Belgium

Tel.: +32-3-2651704

E-mail address: iris.cornet@uantwerpen.be

Abstract

Lignin removal plays a crucial role in the efficient bioconversion of lignocellulose to fermentable sugars. As a delignification process, fungal pretreatment has gained great interest due to its environmental friendliness and low energy consumption. In our previous study, a positive linear correlation between acid-insoluble lignin degradation and the achievable enzymatic saccharification yield has been found, hereby highlighting the importance of the close follow-up of lignin degradation during the solid-state fungal pretreatment process.

However, the standard quantification of lignin, which relies on the two-step acid hydrolysis of the biomass, is highly laborious and time-consuming. Vibrational spectroscopy has been proven as a fast and easy alternative; however, it has not been extensively researched on lignocellulose subjected to solid-state fungal pretreatment. Therefore, the present study examined the suitability of near-infrared (NIR) spectroscopy for the rapid and easy assessment of lignin content in poplar wood pretreated with *Phanerochaete chrysosporium*. Furthermore, the predictive power of the obtained calibration model and the recently published Attenuated Total Reflection Fourier Transform Infrared (ATR-FTIR) spectroscopy-based model was compared for the first time using the same fungus-treated wood data set.

Partial least squares regression (PLSR) was used to correlate the NIR spectra to the acid-insoluble lignin contents (19.9%–27.1%) of pretreated wood. After normalization and second derivation, a PLSR model with a good coefficient of determination (R^2_{CV} = 0.89) and a low root mean square error ($RMSE_{CV}$ = 0.55%) were obtained despite the heterogeneous nature of the fungal solid-state fermentation. The performance of this PLSR model was comparably good to the one obtained by ATR-FTIR (R^2_{CV} = 0.87) while

it required more extensive spectral preprocessing. In conclusion, both methods will be highly useful for the high-throughput and user-friendly monitoring of lignin degradation in a solid-state fungal pretreatment-based biorefinery concept.

Keywords
Biobased economy; Delignification; *Phanerochaete chrysosporium*; Solid-state fermentation; White-rot fungi

1 Introduction

Lignocellulosic biomass derived from plant cell walls is one of the most promising renewable feedstocks for the production of biofuels and biochemicals. However, the genuine recalcitrance of lignocellulose and, consequently, the need to disrupt the cell wall structure to facile access to cellulose and hemicellulose leads to an expensive and challenging conversion process. The presence of lignin in the biomass largely hinders the conversion of carbohydrates to fermentable sugars, both by acting as a physical barrier and binding non-productively to cellulase enzymes during enzymatic saccharification (Rahikainen et al., 2013; Yoo et al., 2020). Pretreatment is a crucial step in improving the efficiency of enzymatic saccharification by removing lignin and reducing the recalcitrance of lignocellulose. Many pretreatment techniques, including alkali, sulfite, organosolv, ionic liquids, deep eutectic solvents, and fungal pretreatment have been evaluated to decrease the lignin content of the biomass prior to enzymatic saccharification. Fungal pretreatment, which mainly uses white-rot fungi for the degradation of lignin, has been widely investigated due to its advantages, such as environmental friendliness, low chemical addition, and lack of the production of inhibiting by-products (Sindhu et al., 2016). Sufficient delignification during fungal pretreatment was proven to greatly improve the conversion of carbohydrates into

fermentable sugars. Moreover, studies reported a positive linear correlation between lignin degradation and the obtained enzymatic saccharification yield, highlighting the significance of delignification and its monitoring during the fungal pretreatment process (Nazarpour et al., 2013; Wittner et al., 2021).

The most widely used method for quantifying lignin in lignocellulose is based on the two-step acid hydrolysis of the biomass (NREL) (Sluiter et al., 2008a). However, this method suffers from the disadvantages of the highly laborious, time-consuming (> 3 h) and destructive procedure and the relatively large sample size (300 mg). These disadvantages can be effectively circumvented by techniques based on infrared spectroscopy. Recently, the study of Wittner et al. demonstrated that Attenuated Total Reflection Fourier Transform Infrared (ATR-FTIR) spectroscopy in the mid-infrared (MIR) region, coupled with partial least squares regression (PLSR) has a high potential to be a fast and accurate analytical tool for predicting lignin content in fungus-treated poplar wood (Wittner et al., 2023). Fackler et al. used both Fourier Transform MIR spectroscopy in transmission mode and Fourier Transform near-infrared (FT-NIR) reflectance spectroscopy to determine lignin content in beech wood before and after fungal decay (Fackler et al., 2007). In their study, the fungal decay of wood was performed in Petri dishes by placing the inoculated beech veneers in water agar and incubating them for up to 10 weeks. However, their application was not aimed at fungal pretreatment and delignification, as in our study. On the contrary, mainly an increase in lignin content was observed, showing that cellulose and hemicellulose compounds were consumed instead. Moreover, NIR spectroscopy has not yet been used for lignin calibration using fungus-treated wood samples obtained by solid-state fermentation (SSF), i.e. in an industry-relevant fungal pretreatment environment (Pandey, 2003; Wan and Li, 2012).

Additionally, the predictive performances of the above-mentioned NIR and ATR-FTIR spectroscopy-based calibration models have not yet been compared based on the same fungus-treated sample set.

Therefore, this study has aimed to achieve the following main research goals. (1) Developing a fast and easy NIR spectroscopy-based lignin determination method using fungus-treated wood samples obtained at optimized solid-state fermentation conditions, hereby opening a new door to the practical implementation of the NIR spectroscopy-based lignin quantification. (2) Investigating the effect of the presence of lignin-degrading enzymes and the fungus itself on the NIR spectra by comparing washed and non-washed pretreated wood samples. (3) Evaluating the use of different spectral preprocessing methods to obtain a PLSR model with a high coefficient of determination and low error for reliable lignin prediction. (4) Comparing the predictive power of the NIR and ATR-FTIR spectroscopy-based calibration models using the same fungus-treated samples to provide important information regarding the right choice of IR instrumentation, spectral data processing and modelling.

Materials and Methods

1.1 Poplar wood substrate and white-rot fungi

Poplar wood sawdust was obtained from Sawmill Caluwaerts Willy (Holsbeek, BE). Sieve analysis was used to determine the particle size distribution of the wood particles. 86.1% w/w of the poplar wood pellets were collected between the 2 mm and 0.075 mm screens. The white-rot fungus *Phanerochaete chrysosporium* MUCL 19343 was used for the solid-state fungal pretreatment studies. A spore suspension of $5 \cdot 10^6$ spores/mL was freshly prepared in distilled water from 5 days old cultures grown on potato dextrose agar plates at 39°C.

1.2 Solid-state fungal pretreatment

In order to obtain fungus-treated wood samples with a sufficient range of variability in AIL content for lignin calibration, the solid-state fermentation (SSF) experiments were carried out at different fermentation conditions as described in the study of Wittner et al. (Wittner et al., 2023). In brief, the fermentations were different in the applied substrate sterilization (none or autoclaving at 121°C for 20 min), duration of fermentation (up to 28 days), medium composition (complex or simple) and fermentation set-up (rolling bottles or trays).

The complex medium was composed of 3 g/L $NaNO_3$, 20 g/L glucose, 0.5 g/L KCl, 0.5 g/L $MgSO_4 \cdot 7H_2O$, 0.5 g/L $FeSO_4 \cdot 7H_2O$, 1 g/L KH_2PO_4, 0.34 g/L veratryl alcohol, 0.1% v/v Tween 80, 3.69 mM $CuSO_4$ and 1.41 mM $MnSO_4$ (Keller et al., 2003; Wittner et al., 2021). The simplified media consisted of 3.69 mM $CuSO_4$, 1.41 mM $MnSO_4$ with or without 20 g/L glucose and/or 3 g/L $NaNO_3$. The Schott bottles (100 mL) contained 3.67 g dry weight (DW) poplar wood, 2 mL sterile media, 3.7 mL spore suspension ($5 \cdot 10^6$ spores/g DW wood) and distilled water, creating a moisture content of 75% w/w on a wet basis. The media and the poplar wood were sterilized separately by autoclavation at 121°C for 20 min. The SSF bottles were rolled on a bottle roller (88881004 Bottle/Tube Roller, Thermo Scientific™) at 4 rpm and incubated (TC 255 S, Tintometer Inc.) at 37°C for up to 4 weeks. Tray fermentations of non-sterilized poplar wood were carried out at 37°C for 4 weeks in 500 mL glass dishes containing 2 mL medium, 2.8 g DW untreated non-sterilized wood, 0.9 g DW pretreated wood as inoculum and distilled water resulting in the moisture content of 75% (Wittner et al., 2023). At the end of the fermentation, the pretreated wood was analyzed for its acid-insoluble lignin (AIL) content by the conventional two-step acid hydrolysis (Sluiter et al., 2008b) as a reference method and

by near-infrared spectroscopy. Table S1 shows the applied medium conditions with the corresponding AIL content for each pretreated wood sample.

1.3 Analytical methods

1.3.1 Removal of water-soluble substances

Prior to the lignin determination, the pretreated wood samples were thoroughly washed to remove the lignocellulolytic enzymes and partially the fungus itself. The washing was carried out as described in the study by Wittner et al. (Wittner et al., 2023). Briefly, the biomass was shaken with 50 mM acetate buffer (pH 4.5) at 400 rpm for 20 min, applying a solid-to-liquid ratio of 1:80, followed by centrifugation (Sigma 3-16KL) for 15 min at 4500 rpm and 4°C. After removing the supernatant, the washing was repeated once with acetate buffer and twice with distilled water to remove the traces of acetic acid. The rinsed solid was freeze-dried (ALPHA 1-2 LDplus, Martin Christ Gefriertrocknungsanlagen GmbH) to a constant weight and used for lignin and infrared analysis.

1.3.2 Lignin quantification

The poplar wood samples, before and after fungal pretreatments, were analyzed for their acid-insoluble content by the standard NREL protocol (NREL/TP-510-42618) (Sluiter et al., 2008b). Briefly, the AIL content of the samples was measured gravimetrically after a two-step acid hydrolysis with sulfuric acid.

1.3.3 Milling

Prior to near-infrared (NIR) analysis, the washed and freeze-dried (Alpha 1-2 LDplus, Martin Christ Gefriertrocknungsanlagen GmbH) wood samples were ground using the method of Cornet et al., with slight modifications (Cornet et al., 2018). The wood samples (200 mg) were placed in a grinding jar (25 mL) containing four 10 mm and one 15 mm stainless steel grinding balls. The jar was cooled down by immersion in liquid nitrogen

for 30 seconds, and ball milling was carried out in a mixer mill (MM 200, Retsch GmbH) for 4 min at 25 Hz.

1.3.3.1 NIR analysis

The milled, freeze-dried wood samples were placed in a powder mini sample holder having a quartz window and an inner ring with a diameter of 6 mm (Foss NIRSystems Inc.) and closed with a disposable sample cup lid (Foss NIRSystems Inc.). The samples were measured in diffuse reflectance mode using a NIR Systems 6500 spectrophotometer (Foss NIRSystems Inc.) equipped with an internal ceramic reference and four PbS detectors. Spectral data were collected between 1100 and 2498 nm at a data interval of 2 nm with 32 scans. Spectra were recorded using Vision 3.20 software (Foss NIRSystems, Inc.).

1.3.4 Spectral data processing and multivariate analysis

All NIR spectra were processed using The Unscrambler® X 10.4 (CAMO Software AS.) and Microsoft® Excel® 2019 (Microsoft Corp.) software. Standard normal variate (SNV) preprocessing was applied to reduce baseline shift (Manfredi et al., 2018). After SNV, principal component analysis (PCA) was carried out on the washed and non-washed wood samples for dimensionality reduction and to identify outlier samples (Sarkar et al., 2017). Since the fungal delignification starts progressively increasing after 14 days of SSF (Wittner et al., 2021), the fermentations carried out longer than 20 days (SSF23–SSF44 in Table S1), were used for the PCA analysis to obtain a good differentiation between the two sample groups (i.e., washed and non-washed). Partial least squares regression (PLSR) models were developed using the acid-insoluble lignin content of the washed SSF samples as reference data (Table S1). PLSR models were built using different spectral pretreatment methods, including the SNV and the second derivative methods of gap-segment (G-S) (also known as Norris-Williams derivative) and Savitzky-Golay (SG)

192 derivative (Rinnan et al., 2009). The gap-segment algorithm generally performs first a
193 smoothing under a given segment size, followed by a derivative of a given order under a
194 given gap size (Kartakoullis et al., 2019). In this study, the use of different segment sizes
195 (1–15 points) at the constant gap size of 1 point was evaluated. The SG algorithm fits
196 polynomials to the spectrum within windows around each point in the spectrum, and these
197 polynomials are then used to smooth the obtained data and subsequently differentiate
198 them (Savitzky and Golay, 1964). Smoothing windows varying from 3 to 15 points were
199 evaluated in this study. Polynomial smoothing involves fitting an odd number of
200 sequential spectral data points to a polynomial and calculating the centre point of the
201 resulting polynomial (McClure, 2008). When using a window that is too wide, peaks and
202 valleys become rounded off, while a narrow window amplifies the noise present in the
203 original spectrum through the derivative calculation (Næs et al., 2002). However, Shenk
204 and Westerhaus suggest that the best mathematical treatment can only be attained by trial
205 and error (Shenk and Westerhaus, 1994).
206 PLSR models were validated using a leave-one-out (i.e. full) cross-validation (CV) to
207 find the best-fitting model that has an optimal combination of the highest coefficient of
208 determination (R^2_{CV}) and the lowest root mean square error of cross-validation ($RMSE_{CV}$)
209 with the lowest number of PLSR terms used.

210 ## 2 Results and Discussion

211 ### 2.1 NIR spectra of fungus-treated wood

212 The NIR spectra of the untreated and pretreated wood with or without washing were
213 compared. The corresponding raw and standard normal variate (SNV) treated second
214 derivative NIR spectra are presented in Fig. 1. SNV is applied to reduce baseline shift
215 caused by light scattering and variable spectral path (Manfredi et al., 2018). Second

derivative spectra have a negative peak that matches exactly the absorption maximum (positive peak) of an absorbance band in log 1/*R*, and these negative peaks are used to detect chemical changes among samples. Second derivative spectra provide more resolved absorption bands and hereby easier band assignments (Czarnecki, 2015) and, therefore, were used in this study for the detailed investigation of spectral changes.

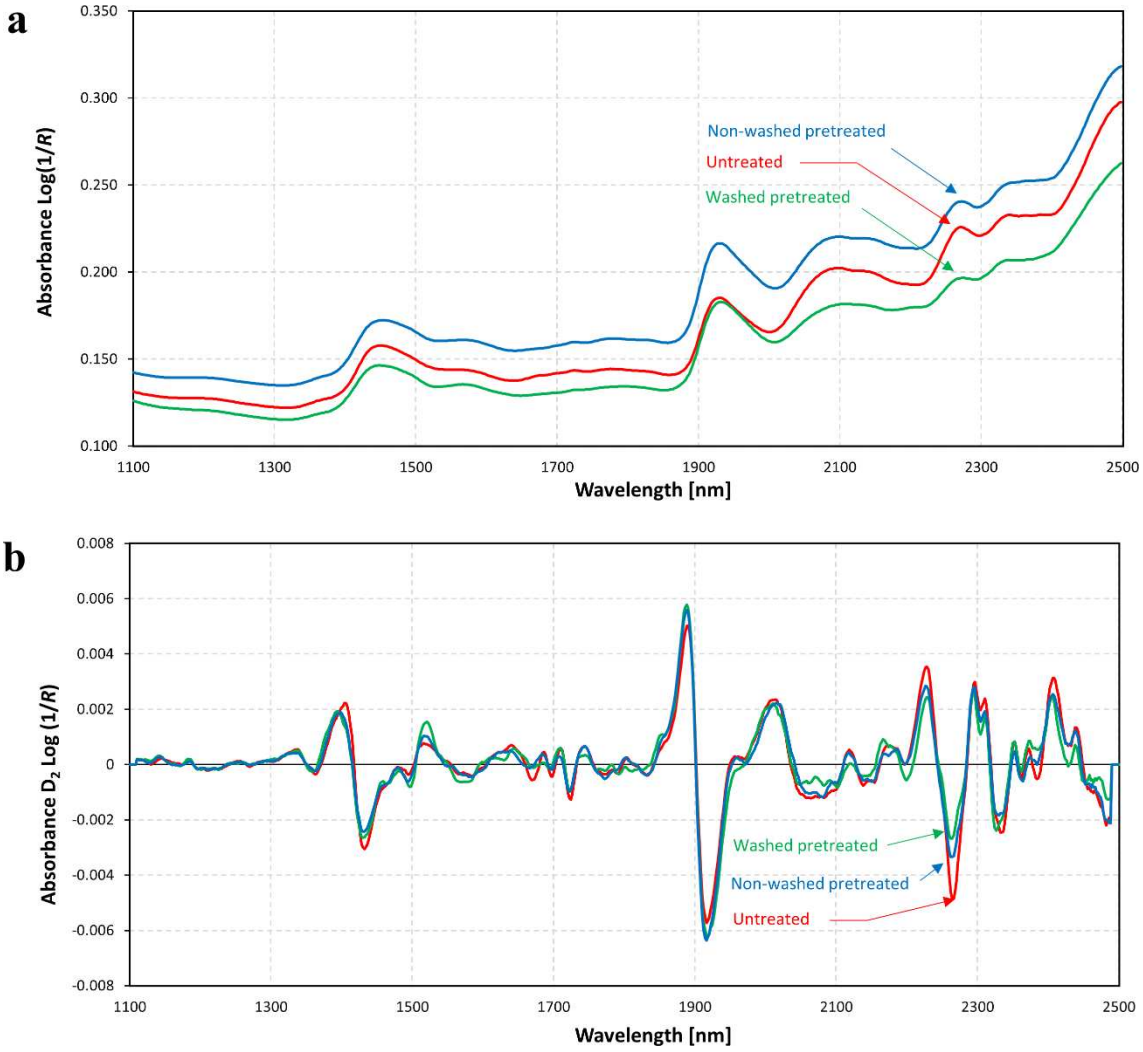

Fig. 1. Raw (a) and Savitzky-Golay second derivative (D_2, 11 smoothing points) of SNV-treated NIR spectra (b) of (—) untreated poplar wood and pretreated poplar wood (—) with and (—) without washing

In the second derivative of SNV-treated spectra, the main changes in the peak intensities after fungal treatment were observed at the lignin-related spectral regions of 1440 nm (1st overtone of C–H stretch and C–H deformation), 1670 nm (1st overtone of aromatic C–H stretch) and 2267 nm (O–H and C–O stretch in lignin), and also at the carbohydrate-dominated regions of 2080 nm (O–H stretch and C–H deformation of semi-crystalline or crystalline regions in cellulose) and 2332 nm (C–H stretch and C–H deformation) (Schwanninger et al., 2011; Yang et al., 2015). The intensity of the lignin-associated peaks decreased after fungal pretreatment, confirming the degradation of lignin moieties. However, the non-washed SSF samples showed a smaller decrease in the lignin-related band intensities than the washed pretreated samples, indicating a spectral interference probably caused by the ligninolytic enzymes and the white-rot fungus, both present in the non-washed sample. The removal of these interfering compounds through washing was confirmed by Bradford protein assay and fungal biomass measurement in the work of Wittner et al. (Wittner et al., 2023). In that study, the same sample set as the one used in this research was measured by ATR-FTIR, and principal component analysis (PCA) was applied to the SNV-treated spectral data (Wittner et al., 2023). The PCA analysis provided a distinct sample group for the washed and non-washed samples. This good differentiation was obtained due to the increased band intensities measured in the non-washed samples in the spectral range of 1700–1500 cm^{-1}, assigned to Amide I and Amide II vibrations originating from the lignin-degrading enzymes and the fungus itself. In comparison, in the NIR spectra, the main influence of the washing was observed at 2267 nm, i.e. at the spectral region, which can also be assigned to proteins besides lignin (Cozzolino, 2021; Shenk et al., 2008) However, unlike in the work of Wittner et al., in this study, no good differentiation could be seen between these sample groups (data not

shown). This can be explained by the increased surface sensitivity and lower optical penetration depth (up to a few micrometres) of ATR-FTIR spectroscopy compared to NIR reflectance spectroscopy (up to a few millimetres) (Cogulet et al., 2016; Lu et al., 2017; Schwanninger et al., 2011). Therefore, ATR-FTIR might be more sensitive to the presence of the ligninolytic enzymes, which cannot penetrate the wood cell wall due to their large size and therefore are deposited on the cell wall surface (Kumar and Chandra, 2020).

2.2 Development of PLSR models for lignin quantification

PLSR was performed to correlate the near-infrared spectra to the acid-insoluble lignin content of 44 wood samples, including the raw feedstock and 43 pretreated wood samples, each obtained via an individual solid-state fermentation (SSF) (Table S1). The acid-insoluble lignin contents of these samples ranged from 19.9% to 27.1%. The PLSR models were constructed using leave-one-out cross-validation. In comparison with the utilization of the raw spectra (R^2_{CV} = 0.79, $RMSE_{CV}$= 0.79%), SNV improved the PLSR model, which was shown by a higher R^2_{CV} of 0.82 and a lower $RMSE_{CV}$ of 0.73% with the same number of PLSR factors (7) (Table 1). In comparison, a higher coefficient of determination (R^2_{CV} = 0.87) and a lower error ($RMSE_{CV}$= 0.60%) were obtained with ATR-FTIR using only 4 PLSR factors and SNV as a preprocessing technique (Wittner et al., 2023).

Table 1. Results of NIR spectroscopy-based PLSR models for lignin quantification

#PLSR model	Treatment	NF [a]	R^2_C [b]	$RMSE_C$ [c] [%]	R^2_{CV} [d]	$RMSE_{CV}$ [e] [%]
PLSR1	raw spectra	7	0.88	0.58	0.79	0.79
PLSR2	SNV	7	0.91	0.51	0.82	0.73
PLSR3	G1-S1	7	1.00	0.08	0.52	1.18

PLSR4	G1-S3	6	0.96	0.33	0.88	0.60
PLSR5	G1-S5	6	0.94	0.40	0.88	0.60
PLSR6	G1-S7	6	0.93	0.43	0.86	0.63
PLSR7	G1-S9	6	0.93	0.45	0.86	0.64
PLSR8	G1-S11	6	0.92	0.48	0.85	0.67
PLSR9	G1-S13	6	0.91	0.51	0.84	0.68
PLSR10	G1-S15	6	0.90	0.52	0.84	0.68
PLSR11	SG3	4	0.96	0.34	0.19	1.53
PLSR12	SG5	7	1.00	0.08	0.63	1.03
PLSR13	SG7	6	0.98	0.26	0.82	0.72
PLSR14	SG9	6	0.97	0.31	0.87	0.61
PLSR15	SG11	6	0.96	0.34	0.88	0.59
PLSR16	SG13	7	0.88	0.58	0.79	0.79
PLSR17	SG15	6	0.94	0.40	0.87	0.60
PLSR18	SNV + G1-S1	4	0.97	0.29	0.50	1.21
PLSR19	SNV + G1-S3	5	0.96	0.35	0.89	0.56
PLSR20	SNV + G1-S5	5	0.93	0.43	0.89	0.58
PLSR21	SNV + G1-S7	5	0.92	0.47	0.87	0.61
PLSR22	SNV + GS-S9	5	0.91	0.50	0.86	0.63
PLSR23	SNV + GS-S11	5	0.90	0.53	0.85	0.66
PLSR24	SNV + GS-S13	6	0.91	0.49	0.85	0.65
PLSR25	SNV + GS-S15	6	0.91	0.50	0.85	0.66
PLSR26	SNV + SG3	3	0.90	0.54	0.19	1.53
PLSR27	SNV + SG5	4	0.98	0.26	0.60	1.07
PLSR28	SNV + SG7	5	0.98	0.24	0.85	0.66
PLSR29	SNV + SG9	5	0.96	0.32	0.89	0.56
PLSR30*	SNV + SG11	5	0.95	0.37	0.89	0.55
PLSR31	SNV + SG13	5	0.94	0.41	0.89	0.56
PLSR32	SNV + SG15	5	0.93	0.43	0.88	0.58

* Spectral pretreatment for which the standardized regression coefficients are shown (Fig. 3).

[a] NF: Number of factors; [b] R_C^2: Coefficient of determination of calibration; [c] $RMSE_C$: Root mean square error of calibration; [d] R_{CV}^2: Coefficient of determination of cross-validation; [e] $RMSE_{CV}$: Root mean square error of cross-validation.

In order to further improve the NIR spectroscopy-based method, the two most common second derivative methods, i.e. the gap-segment (G-S) derivative and Savitzky-Golay (SG) derivative, were tested with or without combining with SNV (Rinnan et al., 2009). Each method (i.e. G-S and SG derivative) requires some trade-off between the amount of

281 sharpening and the creation of artefacts and usually involves some smoothing of the
282 spectra (Hruschka, 2008). The second derivative helps resolve the broad, overlapping
283 bands and peak shoulders and accentuates low-intensity peaks in the NIR region.
284 By using a second derivation, the predictive ability of the PLSR model was efficiently
285 improved. Furthermore, the subsequent use of SNV and second derivation resulted in the
286 best-performing models (Table 1). In the case of the G-S method, the segment size
287 influenced the predictive performance of the model (Table 1). The optimum segment size
288 was 3 points (PLSR19 in Table 1), corresponding to a high determination coefficient of
289 0.89 and a low $RMSE_{CV}$ value of 0.56% using 5 PLSR factors. The utilization of SG
290 second derivative provided similarly good results, i.e. an R^2_{CV} of 0.89 and an $RMSE_{CV}$ of
291 0.55% using 5 factors and the optimal smoothing window of 11 points (PLSR30) (Fig.
292 2). The weighted regression coefficients corresponding to this PLSR model (PLSR30),
293 with the highest coefficient obtained at the lignin-specific wavelength of 2267 nm (O–H
294 and C–O stretching (Schwanninger et al., 2011)), are presented in Fig. 3. Changing the
295 size of the smoothing window had no effect on the location (2267 nm) of the maximum
296 regression coefficient except when using small smoothing windows, i.e. 1 point segment
297 size with G-S method and less than 7 points smoothing window with SG method (Table
298 S2).
299

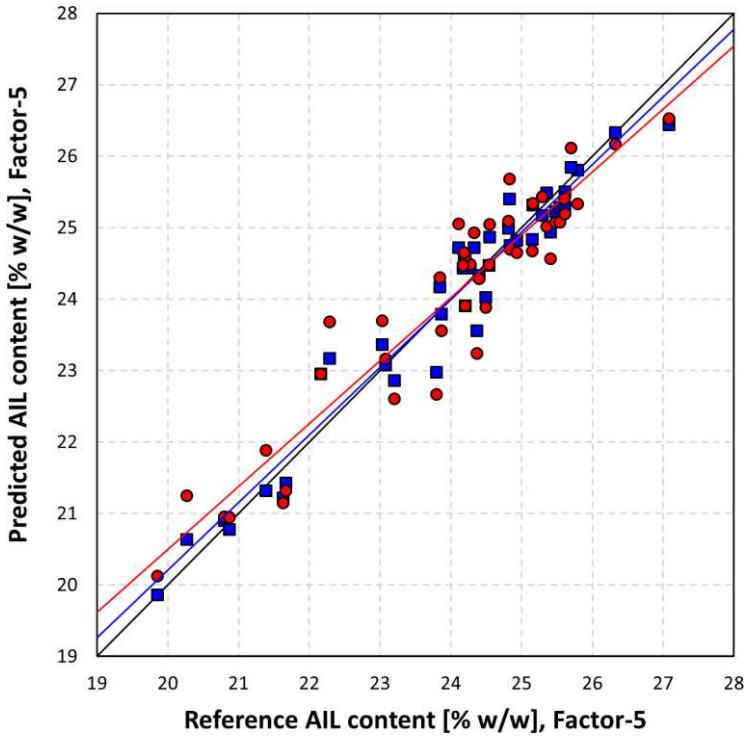

300

301 **Fig. 2.** The predicted vs. reference acid-insoluble lignin (AIL) values of (■) calibration

302 and (●) validation based PLSR30 model in Table 1

303

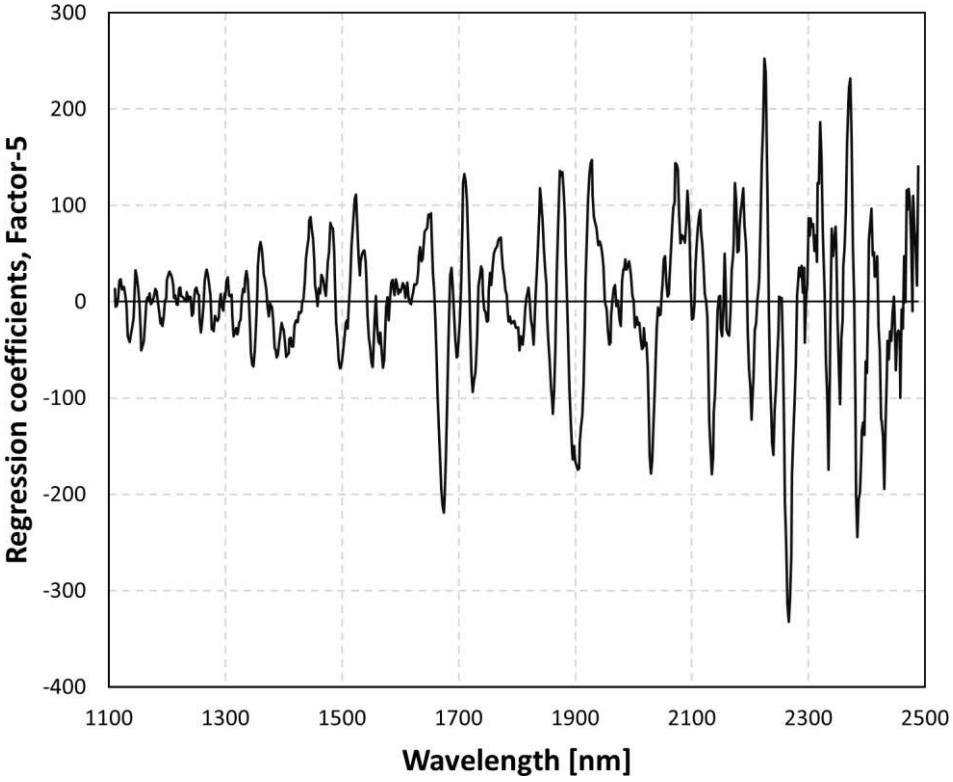

Fig. 3. Regression coefficients of the PLSR30 model (Table 1) for acid-insoluble lignin determination

In comparison to the best-performing PLSR model (PLSR30) obtained in this study, the work of Fackler et al. on the fungal decay of beech wood veneers presented a slightly higher coefficient of determination (R^2_{CV} of 0.91) but also a higher error ($RMSE_{CV}$ = 0.71%) using a higher number of PLSR factors (6) for the NIR spectroscopy-based prediction of lignin in the extracted milled wood samples (Fackler et al., 2007). Additionally, when the model performance of PLSR30 is compared to the ATR-FTIR spectroscopy-based method (R^2_{CV} = 0.87, $RMSE_{CV}$ = 0.60%, 4 PLSR factors (Wittner et al., 2023)), PLSR30 provided a higher coefficient of determination (R^2_{CV} = 0.89) and a lower error ($RMSE_{CV}$ = 0.55%), using 5 PLSR factors. However, NIR spectroscopy required more complex spectral pretreatment, i.e. the combination of SNV and second

318 derivation instead of SNV alone, in order to achieve a coefficient of determination
319 similarly high to the ATR-FTIR method.
320 In conclusion, both NIR spectroscopy and ATR-FTIR spectroscopy showed really good
321 predictive abilities considering the heterogeneous nature of the fungal solid-state
322 fermentation, the different fermentation conditions and the complication of the reference
323 acid-hydrolysis-based method while both are fast, easy and non-destructive methods.

324 ## 3 Conclusions

325 In this study, measuring samples with NIR combined with PLSR succeeded in providing
326 a reliable prediction of acid-insoluble lignin content in poplar wood pretreated by *P.*
327 *chrysosporium* during solid-state fermentation. High correlations (R^2_{CV} = 0.89) between
328 predicted and measured values were obtained with a low error ($RMSE_{CV}$ = 0.55%) using
329 5 PLSR components. The performance of this PLSR model was comparable to the one
330 obtained by ATR-FTIR (R^2_{CV} = 0.87, $RMSE_{CV}$ = 0.60%, 4 PLSR factors), while it required
331 the combined application of SNV and second derivation instead of SNV alone. In
332 conclusion, both methods are highly suitable for the use as fast and easy lignin
333 quantification in fungus-treated biomass in a wood-based biorefinery concept.

334 ## Appendix A. Supplementary data

335 E-supplementary data of this work can be found in the online version of the paper.

336 ## Acknowledgements

337 This research has been funded by the University of Antwerp (Project number: 36691) and
338 by the European Union (Project number: RRF-2.3.1-21-2022-00015).

339 ## References

340 Cogulet, A., Blanchet, P., Landry, V., 2016. Wood degradation under UV irradiation: A
341 lignin characterization. J. Photochem. Photobiol. B Biol. 158, 184–191.
342 https://doi.org/10.1016/J.JPHOTOBIOL.2016.02.030

Cornet, I., Wittner, N., Tofani, G., Tavernier, S., 2018. FTIR as an easy and fast analytical approach to follow up microbial growth during fungal pretreatment of poplar wood with Phanerochaete chrysosporium. J. Microbiol. Methods 145, 82–86. https://doi.org/10.1016/J.MIMET.2018.01.004

Cozzolino, D., 2021. The Ability of Near Infrared (NIR) Spectroscopy to Predict Functional Properties in Foods: Challenges and Opportunities. Molecules 26. https://doi.org/10.3390/MOLECULES26226981

Czarnecki, M.A., 2015. Resolution enhancement in second-derivative spectra. Appl. Spectrosc. 69, 67–74. https://doi.org/10.1366/14-07568

Fackler, K., Schwanninger, M., Gradinger, C., Hinterstoisser, B., Messner, K., 2007. Qualitative and quantitative changes of beech wood degraded by wood-rotting basidiomycetes monitored by Fourier transform infrared spectroscopic methods and multivariate data analysis. FEMS Microbiol. Lett. 271, 162–169. https://doi.org/10.1111/j.1574-6968.2007.00712.x

Hruschka, W.R., 2008. Spectral Reconstruction, in: Handbook of Near-Infrared Analysis. 3rd Ed. (Ed. Burns. CRC Press, pp. 333–344. https://doi.org/10.1201/9781420007374-22

Kartakoullis, A., Comaposada, J., Cruz-Carrión, A., Serra, X., Gou, P., 2019. Feasibility study of smartphone-based Near Infrared Spectroscopy (NIRS) for salted minced meat composition diagnostics at different temperatures. Food Chem. 278, 314–321. https://doi.org/10.1016/J.FOODCHEM.2018.11.054

Keller, F.A., Hamilton, J.E., Nguyen, Q.A., 2003. Microbial Pretreatment of Biomass. Biotechnol. Fuels Chem. 105, 27–41. https://doi.org/10.1007/978-1-4612-0057-4_3

Kumar, A., Chandra, R., 2020. Ligninolytic enzymes and its mechanisms for degradation of lignocellulosic waste in environment. Heliyon 6, e03170. https://doi.org/10.1016/J.HELIYON.2020.E03170

Lu, Z., DeJong, S.A., Cassidy, B.M., Belliveau, R.G., Myrick, M.L., Morgan, S.L., 2017. Detection Limits for Blood on Fabrics Using Attenuated Total Reflection Fourier Transform Infrared (ATR FT-IR) Spectroscopy and Derivative Processing. Appl. Spectrosc. 71, 839–846. https://doi.org/10.1177/0003702816654154

Manfredi, M., Robotti, E., Quasso, F., Mazzucco, E., Calabrese, G., Marengo, E., 2018. Fast classification of hazelnut cultivars through portable infrared spectroscopy and chemometrics. Spectrochim. Acta Part A Mol. Biomol. Spectrosc. 189, 427–435. https://doi.org/10.1016/J.SAA.2017.08.050

McClure, W.F., 2008. Analysis Using Fourier Transforms, in: Handbook of Near-Infrared Analysis. 3rd Ed. (Ed. Burns, D.A., Ciurczak, E.W.). CRC Press, pp. 93–121. https://doi.org/10.1201/9781420007374-11

Næs, T., Isaksson, T., Fearn, T., Davies, T., 2002. Scatter correction of spectroscopic data., in: A User-Friendly Guide to Multivariate Calibration and Classification. IM Publications Open, pp. 105–125. https://doi.org/https://doi.org/10.1002/cem.815

Nazarpour, F., Abdullah, D.K., Abdullah, N., Zamiri, R., 2013. Evaluation of biological pretreatment of rubberwood with white rot fungi for enzymatic hydrolysis. Materials (Basel). 6, 2059–2073. https://doi.org/10.3390/ma6052059

Pandey, A., 2003. Solid-state fermentation. Biochem. Eng. J. 13, 81–84. https://doi.org/10.1016/S1369-703X(02)00121-3

Rahikainen, J.L., Evans, J.D., Mikander, S., Kalliola, A., Puranen, T., Tamminen, T., Marjamaa, K., Kruus, K., 2013. Cellulase–lignin interactions—The role of carbohydrate-binding module and pH in non-productive binding. Enzyme Microb. Technol. 53, 315–321. https://doi.org/10.1016/J.ENZMICTEC.2013.07.003

Rinnan, Å., Berg, F. van den, Engelsen, S.B., 2009. Review of the most common pre-processing techniques for near-infrared spectra. TrAC Trends Anal. Chem. 28, 1201–1222. https://doi.org/10.1016/J.TRAC.2009.07.007

Sarkar, S., Taraphder, U., Datta, S., Swain, S.P., Saikhom, D., 2017. Multivariate Statistical Data Analysis-Principal Component Analysis (PCA). Int. J. Livest. Res. 7, 60–78. https://doi.org/10.5455/ijlr.20170415115235

Savitzky, A., Golay, M.J.E., 1964. Smoothing and Differentiation of Data by Simplified Least Squares Procedures. Anal. Chem. 36, 1627–1639. https://doi.org/10.1021/AC60214A047/ASSET/AC60214A047.FP.PNG_V03

Schwanninger, Manfred, Rodrigues, José Carlos, Fackler, Karin, Schwanninger, M, Rodrigues, J C, Fackler, K, 2011. A review of band assignments in near infrared spectra of wood and wood components Special Issue on Wood and Wood products. J. Near Infrared Spectrosc 19, 287–308. https://doi.org/10.1255/jnirs.955

Shenk, J.S., Westerhaus, M.O., 1994. The Application of near Infrared Reflectance Spectroscopy (NIRS) to Forage Analysis, Forage Quality, Evaluation, and Utilization. John Wiley & Sons, Ltd. https://doi.org/https://doi.org/10.2134/1994.foragequality.c10

Shenk, J.S., Workman, J.J.J., Westerhaus, M.O., 2008. Application of NIR spectroscopy to agricultural products, Handbook of near-infrared analysis. 3rd ed. (ed. Burns, D.A., Ciurczak, E.W.). CRC Press. https://doi.org/https://doi.org/10.1201/9781420007374-24

Sindhu, R., Binod, P., Pandey, A., 2016. Biological pretreatment of lignocellulosic biomass – An overview. Bioresour. Technol. 199, 76–82. https://doi.org/10.1016/J.BIORTECH.2015.08.030

Sluiter, A., Hames, B., Ruiz, R., Scarlata, C., Sluiter, J., Templeton, D., Crocker, D., 2008a. Determination of Structural Carbohydrates and Lignin in Biomass: Laboratory Analytical Procedure (LAP) (Revised August 2012).

Sluiter, A., Ruiz, R., Scarlata, C., Sluiter, J., Templeton, D., 2008b. Determination of Extractives in Biomass: Laboratory Analytical Procedure (LAP).

Wan, C., Li, Y., 2012. Fungal pretreatment of lignocellulosic biomass. Biotechnol. Adv. 30, 1447–1457. https://doi.org/10.1016/J.BIOTECHADV.2012.03.003

Wittner, N., Broos, W., Bauwelinck, J., Slezsák, J., Vlaeminck, S.E., Cornet, I., 2021.

425 Enhanced fungal delignification and enzymatic digestibility of poplar wood by
426 combined CuSO4 and MnSO4 supplementation. Process Biochem. 108, 129–137.
427 https://doi.org/10.1016/J.PROCBIO.2021.06.002

428 Wittner, N., Slezsák, J., Broos, W., Geerts, J., Gergely, S., Vlaeminck, S.E., Cornet, I.,
429 2023. Rapid lignin quantification for fungal wood pretreatment by ATR-FTIR
430 spectroscopy. Spectrochim. Acta Part A Mol. Biomol. Spectrosc. 285, 121912.
431 https://doi.org/10.1016/J.SAA.2022.121912

432 Yang, Z., Liu, Y., Pang, X., Li, K., 2015. Preliminary Investigation into the
433 Identification of Wood Species from Different Locations by Near Infrared
434 Spectroscopy. BioResources 10, 8505–8517.

435 Yoo, C.G., Meng, X., Pu, Y., Ragauskas, A.J., 2020. The critical role of lignin in
436 lignocellulosic biomass conversion and recent pretreatment strategies: A
437 comprehensive review. Bioresour. Technol. 301, 122784.
438 https://doi.org/10.1016/J.BIORTECH.2020.122784

439